

Pressure Field Generated by Jet-on-Jet Impingement

Nagy Nosseir,* Uri Peled,† and Gregory Hildebrand†
San Diego State University, San Diego, California

The impingement of two axisymmetric turbulent jets on each other is investigated experimentally. The angle of impingement is equal to 180 deg and the jets are issued from large flat plates. Characteristics of the flowfield and pressure disturbances generated in the impinging region and amplified by the feedback mechanisms are discussed.

Nomenclature

| | |
|--------------|---|
| a_0 | = speed of sound |
| C_p | = pressure coefficient, $= p' / \frac{1}{2} \rho U^2$ |
| f | = frequency, Hz |
| H | = distance between the exit planes of the jets |
| K | $= \frac{1}{2} \rho U^2 [(r_j/H)(r_j/L)]^2$ |
| L | = radius of the plate |
| M | = Mach number, $= U/a_0$ |
| P | = mean surface pressure |
| p' | = rms of surface pressure fluctuation |
| r, ϕ, z | = cylindrical coordinate system |
| r_j | = jet exit radius, $= 4.87$ cm |
| r_0 | = radial distance along the plate |
| r_r | = radial distance of reattachment |
| St | = Strouhal number, $= f(2r_j)/U$ |
| T | = averaging time for rms values (e.g., p') |
| U | = jet exit velocity |
| τ_0 | = delayed time of the optimum correlation peak |

Introduction

THE head-on collision of two high-speed jets is an interesting fluid mechanics research subject that has not been fully addressed in the literature. The flowfield is made up of a number of diverse flow modules. The theoretical model proposed by Powell¹ can be used as a first step in understanding these modules. Powell's mirror image concept suggests that the impingement of two jets, separated by a distance H , on each other is equivalent to the impingement of one of the jets on a flat plate placed at a distance $H/2$ downstream. Accordingly, if the jets are axisymmetric, the flowfield would be axisymmetric and would include free jets, jet-jet impingement, jet-solid-boundary interaction in the reattachment region, and circulating flow in the separation bubbles formed between each jet lip and the reattachment region. Each of these flow modules would contribute to the pressure field generated in this flowfield. Furthermore, pressure oscillations can be amplified due to a coupling between two or more of these modules.

From a practical point of view, the impingement of free jets on each other is an important feature of the flowfield inside a side-dump ramjet combustor. In this combustor, premixed air-fuel jets are introduced in the combustor through ports in its side. Fluid mixing and the combustion process take place primarily in the impinging region of the jets. Several current ramjet engines exhibit high-amplitude, combustion-induced pressure oscillations. Based on results

from ground testing,² the frequencies of pressure oscillations are categorized into very low frequency (or buzz), low frequency, and high frequency (or screech). Among these categories, the low-frequency oscillations (in the range 200–500 Hz) poses the most serious problem in the development of these engines. The root mean square (rms) of the oscillation amplitudes can reach up to 20% of the combustor's static pressure.^{3,4} In addition, pressure disturbances generated during the combustion can propagate upstream and interact with the inlet shock wave, causing inlet unstarting as well as degraded engine performance. Flow-induced pressure oscillations due to jet-jet impingement is one of several mechanisms suspected of triggering combustion instabilities. Therefore, understanding of jet-jet impingement is important in achieving good combustion performance as well as arriving at possible solutions to combustion instabilities.

The adoption of Powell's model as a first step in the study of jet-jet impingement implies that pressure oscillations and their generating mechanisms are similar to those of jet-plate impingement. High-amplitude pressure oscillations in jet-plate impingement were investigated experimentally by Ho and Nosseir.⁵ A feedback of pressure waves between the nozzle and the plate was the generating mechanism. The feedback loop consisted of downstream-traveling pressure waves induced by the coherent structures of the turbulent jet and upstream-traveling pressure waves generated by the impingement of the coherent structures on the plate. The propagation speed of the upstream-traveling waves was measured and found to be equal to the speed of sound in the quiescent region of the jet. (Based on flow visualization of standing waves in the jet core, Neuwerth⁶ argued that the upstream propagation of pressure waves rather occurs inside the jet core). The feedback loop was completed by the pressure waves forcing the shear layer at the nozzle lip to roll up into new coherent structures.

Powell's mirror image concept is plausible if the impinging jets are laminar. However, the instabilities associated with the free jets upstream of their impingement cast serious doubts on the validity of the concept in a turbulent flowfield. Indeed, recent flow visualization⁷ has indicated that jet column oscillations occurred when two rectangular water jets impinged on each other. The frequency of the oscillations scaled with the jet velocity U and the distance H between the jets.

The present experiment is part of an investigation into flow-induced oscillations in side-dump ramjet combustors. An axisymmetric configuration is being considered in the present experiment in which the two jets are issued from large, parallel plates. In this way, the impingement of two turbulent jets on each other is isolated from effects due to the geometry of the combustor. Our objectives are to study 1) the behavior of the jets as they impinge on each other, 2) the pressure field generated by the impingement,

Received Sept. 29, 1986; revision received Dec. 16, 1986.
 Copyright © American Institute of Aeronautics and Astronautics, Inc., 1987. All rights reserved.

*Associate Professor. Member AIAA.

†Research Assistant. Member AIAA.

and 3) the mechanisms of the dominant pressure oscillations.

Experimental Facilities

The SDSU supersonic windtunnel was modified for the present experiment (Fig. 1). In this facility, a compressor (Joy, model WL 80B-100H) supplies the air to the storage pressure vessel prior to each test run. The air flows from the pressure vessel into a stilling chamber fitted with screens to reduce the turbulence level. The stagnation pressure in the stilling chamber is regulated by a low-noise, self-drag valve (Fisher, model E-470). Downstream of the stilling chamber, the air is divided and flows through two pipes, each fitted with a choked converging-diverging nozzle. The choked nozzles are used to resemble actual inlet operation in ramjet engines. The air then flows through 90 deg elbows before it exits from the pipes. The exit planes of the pipes are flush-mounted on two parallel flat plates. The area of each plate is approximately 100 times larger than the cross-sectional area of the pipe so that edge effects on the jet-jet impingement are minimized. Restricted ambient entrainment to the jets due to the presence of the infinitely large plates is chosen in this experiment to resemble the situation in a ramjet combustor.

The propagation of flow-induced disturbances was measured by pressure transducers (Kulite model XCW-190-15) that were flush-mounted on the plates. Analyses of the pressure signals were conducted using a two-channel analyzer (Spectral Dynamics model SD 375).

An important feature to the understanding of the fundamentals of jet-jet impingement is the axisymmetry of the flowfield. Therefore, it was important for the velocity profiles at the exit planes of the jets to be uniform. The velocity profile of the jet (Fig. 2) exhibited a strong gradient due to centrifugal forces exerted on the fluid at the elbows. Since the jet exited from the pipe a short distance (approximately 12 cm) downstream of the elbow, the conventional method of installing vanes in the elbows was unsuccessful in achieving a uniform velocity profile. A system of a half screen covering the outer part of the pipe cross-sectional area and a full screen sandwiching a honeycomb was used in the experiment and rendered a uniform velocity profile as is shown in Fig. 2. The two jets were carefully matched so that the difference between the velocities at the exit planes of the jets was within 4% of the average speed of 100 m/s.

Two methods were used for flow visualization. China clay paint, a suspension of kaolin in kerosene, was used as a surface tracer and tufts were used to trace the flow between the plates (Fig. 3). Each tuft was glued to a thin plastic disk having a small hole. A thin wire (2 mm in diameter) was threaded through the disk's hole. Small pieces of rubber were placed above and below the disk to restrict its motion along the wire. Several tufts were positioned approximately every 1.8 cm along the wire. The wire was stretched vertically between

the plates (Fig. 3). In this way, the tufts were free to rotate about the wire in horizontal planes, i.e., $z = \text{const}$. Several wires were used to visualize the flow pattern in cross-sectional planes, i.e., $\phi = \text{const}$. In particular, video movies were taken of the flow in the $\phi = 0$ and 90 deg planes. Figure 3 also shows the cylindrical coordinates (r, ϕ, z), with the two jet pipes being in the $\phi = 0$ deg plane.

Experimental Results

Characteristics of the Flowfield

The head-on impingement of the two jets was highly unstable. Flow visualization indicated that the jets oscillated due to their impingement. The average period of oscillation laid in the range of 0.5–1 s. Based on visualization of the flow in a cross-sectional plane, i.e., $\phi = \text{const}$, two modes of oscillations were observed: a symmetrical mode and an antisymmetrical mode. In the symmetrical mode, the instantaneous streamline pattern (Fig. 4a) indicated that the flow reattached to the upper plate and an open separation bubble was formed over the lower plate, i.e., the flow did not reattach to the lower plate. In the other half of the oscillation cycle of this mode, the flow reattached to the lower plate

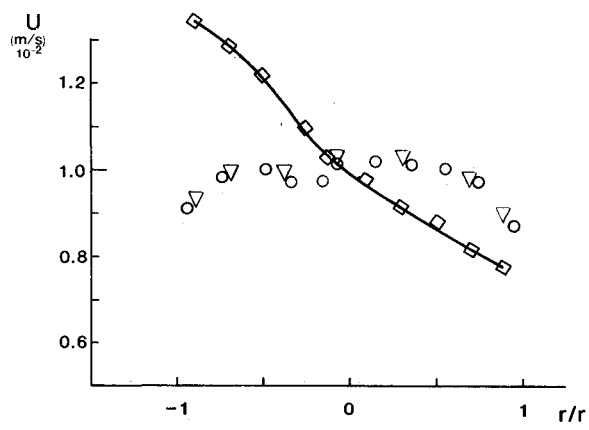


Fig. 2 Velocity profiles at the exit planes of the upper jet \diamond without screens or honeycomb; upper jet \circ and lower jet ∇ after the addition of a half-screen/honeycomb/full screen combination downstream of the 90 deg elbow.

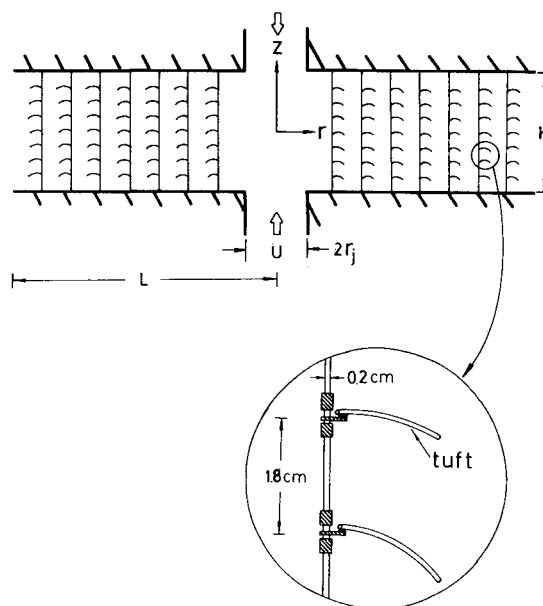


Fig. 3 Schematic of jet-jet impingement and the arrangement of tufts for flow visualization.

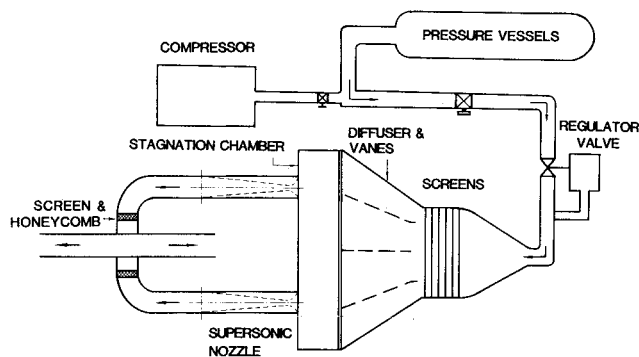


Fig. 1 SDSU supersonic tunnel after modifications to study ramjet combustion instabilities.

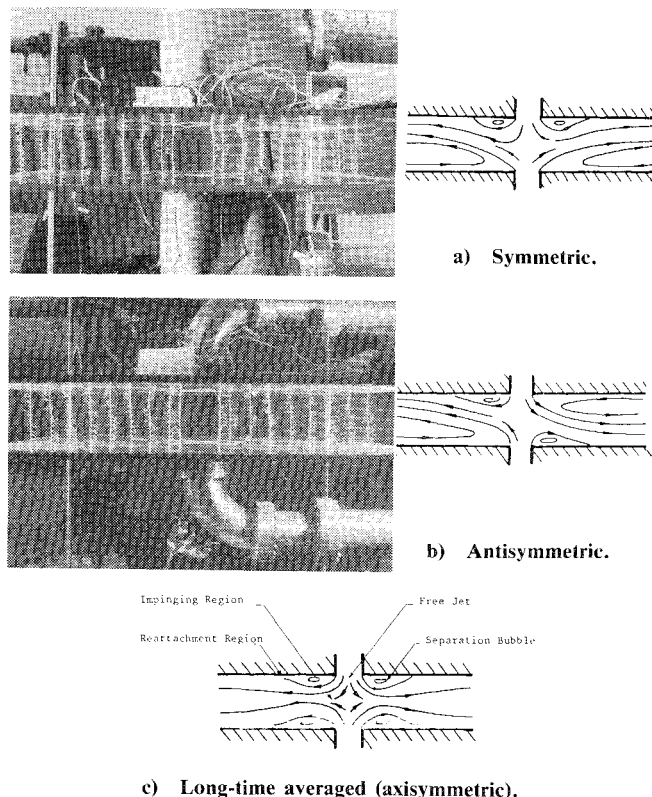


Fig. 4 Modes of oscillation of the impinging jets. The instantaneous streaklines patterns in a) and b) are constructed from the tuft photographs. Flow modules according to Powell's mirror image concept¹ are indicated in c).

while the open separation bubble moved to the upper plate. In the antisymmetric mode (Fig. 4b), the jets were deflected in opposite directions. In Fig. 4b, for example, the flow reattached to the left side of the upper plate, while an open separation bubble was formed on the right side of the lower plate. The two modes of oscillation were observed to occur simultaneously in two perpendicular planes approximately 90% of the time.

It should be noted that the above modes were observed after a painstaking process of aligning the two axes of the jets. Our guide to the final alignment was the random oscillations of the flow as indicated by the tufts. Furthermore, pictures with a long-time exposure of the flow revealed an axisymmetric flowfield, as would have been predicted by the mirror image concept. This was further confirmed by the circular reattachment contour that was visualized over one of the plates by the china clay paint (Fig. 5). In this case, $H = 20$ cm, the radius of the reattachment circle was equal to 20 cm.

The effect of the plates' dimensions on the flowfield was examined by replacing the original plates, 91×91 cm in dimension, by disks of radius $L = 61$ cm. Pressure fluctuations, which will be discussed later, with frequencies higher than jet oscillation, i.e., $f \gg 1$ Hz, were not significantly altered. However, surface tufts indicated that the flow reattached axisymmetrically to the upper plate with an open separation bubble forming on the lower plate (as in Fig. 4a). Whenever we introduced a disturbance in the impinging region, e.g., a pitot-static tube, the flow would reattach to the lower plate instead. This phenomenon was previously observed in similar flows under strong adverse pressure gradients. In two-dimensional diffusers, the flow experiences "transitory" stall depending on the divergence angle and the aspect ratio of the diffuser.⁸ In transitory stall, the flow discriminately separates from one side of the diffuser despite

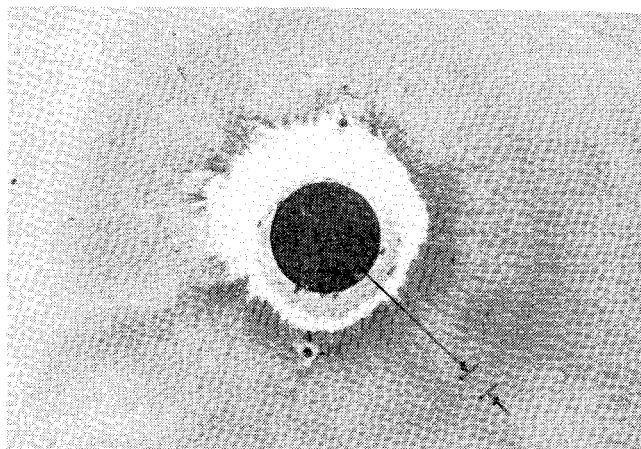


Fig. 5 Circular reattachment region is indicated on the lower plate by China clay, a suspension of kaolin in kerosene.

the symmetry of the diffuser walls with respect to the centerline plane.

Characteristics of the Pressure Field

Surface pressure fluctuations represent the footprints of the flow structures traveling radially between the plates. The radial variation of the time-averaged surface pressure P is shown in Fig. 6. The pressure decreases to a minimum and then increases monotonically to zero (i.e., atmospheric pressure) at the outer edges of the plates. This trend was obtained only after long time averaging ($T \gg 1$ s), since the pressure signal was dominated by high-amplitude fluctuations. The amplitude of fluctuations reached up to 40% of the mean pressure at the minimum pressure point $r_0 = 22$ cm (as is indicated by the vertical bar in Fig. 6). As expected, the strong pressure fluctuations were due to oscillations of the jet columns which were discussed earlier. Also, in a low Reynolds number experiment,⁷ flow visualization indicated that the impingement of the side jets of a combustor on each other has caused their columns to oscillate. The period of the oscillations was equal to approximately $H/0.3U$. Since the measured pressure was typically averaged over a time much larger than the characteristic period of oscillations, axisymmetry of the flow-induced pressure was recovered. Therefore, the pressure variation in Fig. 6 can be explained as follows. Each jet separated from the plate at its exit plane. Upon impinging on the other jet, the flow reattached to the plate and continued to travel radially outward. According to the continuity equation, the average radial speed of the flow increased first as the two jets impinged on each other. Downstream of reattachment, the speed decreased as the flow spread outward. Therefore, the average static pressure according to Bernoulli's equation, first decreased to the reattachment region and then increased to zero.

According to continuity, the radial velocity downstream of the reattachment is equal to $U(r_j/H)(r_j/r)$ and the radial pressure variation by Bernoulli's equation is given by

$$P = K[1 - (L^2/r^2)]$$

where $K = \frac{1}{2}\rho U^2 [(r_j/H)(r_j/L)]^2$. The above equation agreed well with the measured pressure downstream of reattachment (Fig. 6). Also, the highest pressure fluctuations occurred in the reattachment region at $r_0 = 22$ cm, which is approximately equal to the radius of the reattachment circle visualized in Fig. 5.

Effects of the distance between the jets H on the non-dimensional root mean square of the surface pressure fluctuation, $C_p = p'/\frac{1}{2}\rho U^2$, is shown in Fig. 7. The amplitude of the fluctuations decreased with increasing H . For $H < 2.6r_j$,

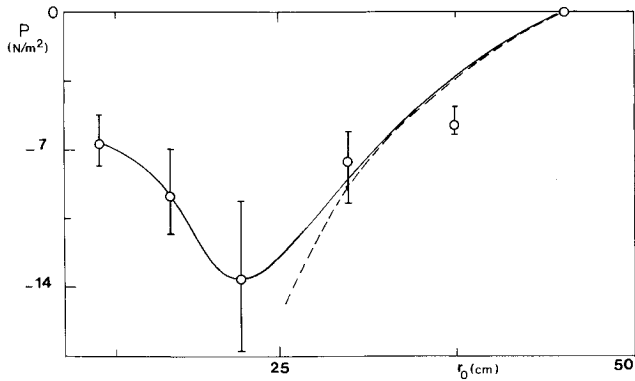


Fig. 6 Radial variation of surface pressure (upper plate) ($H=15.24$ cm, $\phi=90$ deg). The inviscid solution, $P=K(1-L^2/r^2)$, is indicated by a broken line.

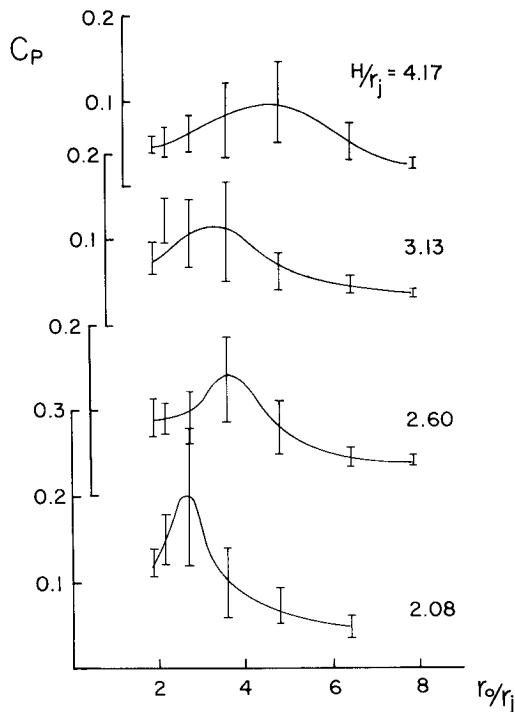


Fig. 7 Radial variation of the rms of the pressure fluctuation. Vertical bars represent the limits reached if shorter time averaging is considered.

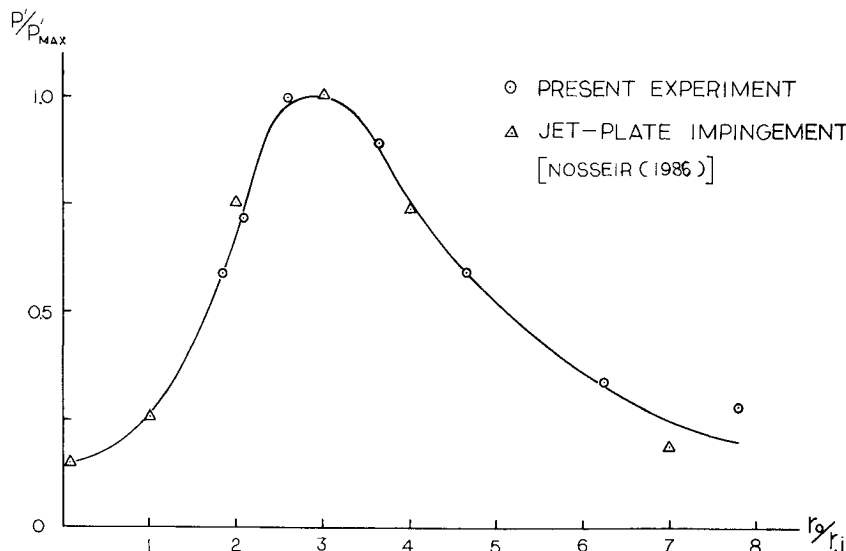


Fig 8 Normalized surface pressure fluctuation: \circ jet-jet impingement ($H=4$ in.) and \triangle jet-plate impingement (jet-to-plate distance is two jet diameters).

the reattachment region at which the highest fluctuation occurred moved outward with increasing H . However, at larger H , the reattachment radius appeared to be independent of H and equal to approximately $3.3r_j$. This could be due to failure of the flow to fill the radial space between the plates, as was indicated by the flow visualization. The pressure fluctuations were reduced at the outer part of the plates and their radial variation was independent of H . In this region, the surface pressure is that of a wall jet which through viscous dissipation tends to “forget” its past history.

The above characteristics of the surface pressure fluctuations are similar to those measured in a jet impinging on a flat plate.⁹ For a nozzle-to-plate distance less than the length of the jet potential core, p' increases radially to a maximum at a location where the large-scale structures of the jet impinge on the plate. Downstream of the impingement region, p' decreases asymptotically to a value corresponding to the wall jet. According to the mirror image concept, the same radial variation of p' would be measured on a plate placed a distance equal to $H/2$ from either jet in the present configuration. Since it can be assumed that the pressure is impressed on the plates, i.e.,

$$\frac{\partial p'}{\partial z} \ll \frac{\partial p'}{\partial r}$$

a similarity in the radial variation of p' in both configurations is expected. In Fig. 8 the radial variation of the normalized pressure fluctuation is shown to compare well with its counterpart in the jet-plate impingement.⁹ It should be pointed out that the normalized p' distribution show a qualitative similarity between the two configurations; however, C_p is larger in the present configuration. The reason is the superimposed fluctuations associated with reattachment.

Generated Tones

The spectra of the pressure signals exhibited several peaks (Fig. 9). The frequencies (in hertz) of the dominant peaks are listed in Fig. 10. In this figure, the nondimensional Strouhal number, $St=f(2r_j)/U$, is plotted against the distance between the jets. Based on Fig. 10, the dominant tones can be categorized as high frequency and low frequency. The high-frequency tones varied with the distance H ; however, the low-frequency tones (at 220 and 515 Hz) were independent of H .

Generation of High-Frequency Tones

The cross-correlation function of the pressure signals from two transducers opposite each other on the plates (Fig. 11),

where $H = 20$ cm, indicates an optimum peak with a delayed time $\tau_0 = -0.057$ ms. Accordingly, the propagation speed of the pressure fluctuation between the plates is equal to a_0 , approximately. Therefore, the resonant frequency of the acoustic field between the plates should satisfy the standing wave relation,¹⁰

$$2\pi f_h = (a_0/H) (N\pi) \quad (1)$$

where $N = 1, 2, \dots$. The measured high-frequency tones (Fig. 10) are in excellent agreement with the frequencies predicted by Eq. (1).

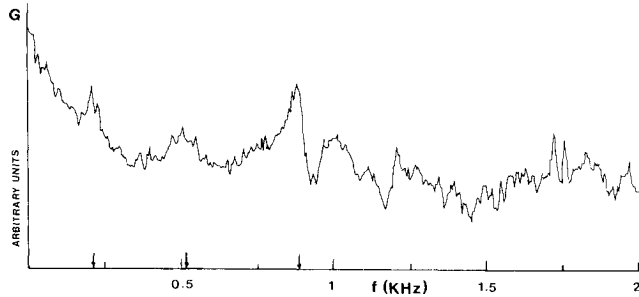


Fig. 9 Power spectrum of surface pressure fluctuation ($r_0 = 8.9$ cm, $H = 20.3$ cm).

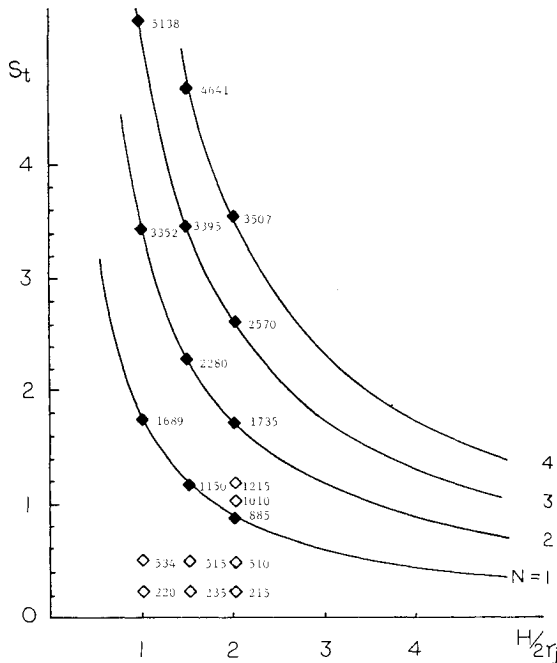


Fig. 10 Variation of the high-frequency, resonant Strouhal number, $St = f_h(2r_j)/U$, with nondimensional distance between the jets: \diamond measured — calculated from Eq. (1), \circ measured low frequencies independent of H . The frequency in hertz is indicated to the right of each data point.

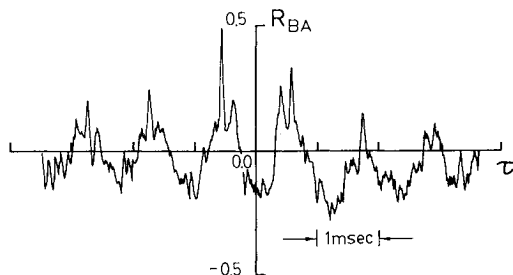


Fig. 11 Cross-correlation between two transducers at $r_0 = 10$ cm, A on the upper plate and B on the lower.

The main features of the correlation in Fig. 11 can be further explained in light of the excellent agreement between Eq. (1) and the measured high-frequency tones. The period of the correlation's oscillation corresponds to the fundamental frequency at 885 Hz. The correlation has minima at $\tau = 0$, which corresponds to a phase angle between the pressure fluctuations at the plates equal to π in agreement with $N = 1$ in Eq. (1). Furthermore, since pressure waves reflected from the plates are not expected to be equal to the incident waves, a propagating component of the pressure waves would be superimposed on the standing waves. This would cause, for example, the pressure at a node not to be equal to zero. Accordingly, the correlation exhibits optimum peaks at $\tau = \pm 0.057$, which corresponds to the propagation of waves between the plates.

Generation of the Low-Frequency Tones

The tones (at 220 and 515 Hz) are associated with characteristic lengths that are unchanged with changing the distance H between the plates. Pressure disturbances generated in the impinging region near the jet axes are expected to propagate radially to the outer edge of the plates, $r_0 = L$, where the boundary conditions are fixed at $P = 0$. The radial propagation of the pressure can be described by the wave equation in cylindrical form,¹⁰

$$\frac{\partial^2 p}{\partial t^2} = a_0^2 \left(\frac{\partial^2 p}{\partial r^2} + \frac{1}{r} \frac{\partial p}{\partial r} + \frac{1}{r^2} \frac{\partial^2 p}{\partial \phi^2} + \frac{\partial^2 p}{\partial z^2} \right)$$

which, assuming a small variation of p in the z direction reduces to

$$\frac{\partial^2 p}{\partial t^2} = a_0^2 \left(\frac{\partial^2 p}{\partial r^2} + \frac{1}{r} \frac{\partial p}{\partial r} + \frac{1}{r^2} \frac{\partial^2 p}{\partial \phi^2} \right) \quad (2)$$

Equation (2) also describes the vibration of a circular membrane of radius L . The natural frequencies predicted by Eq. (2) are given by

$$J_m [2\pi f_{m,n} (L/a_0)] = 0 \quad (3)$$

where J_m is the Bessel function of n th order. The boundary condition of $P(L, \phi, t) = 0$ is included in Eq. (3). The fundamental frequency ($m = 1, n = 0$) according to Eq. (3) is

$$2\pi f_{1,0} = 2.4 (a_0/L) \quad (4)$$

For $L = 61$ cm, Eq. (4) predicts a value of $f_{1,0} = 218$ Hz, which is equal to the measured frequency.

A convective resonance model is proposed to explain the generation of the 520 Hz tone. The model is supported by two observations:

1) Due to the high level of pressure fluctuation measured in the reattachment region, a "virtual" sound source can be assumed at $r_0 = r_r$. The pressure fluctuation is generated by the interaction of the coherent structure of the jets with the plates. In a two-dimensional flow over a backward facing step, Troutt et al.¹¹ found that the spatial fluctuation of the reattachment point was strongly correlated with the passage frequency of the coherent structure of the shear layer. Also, Eaton and Johnston¹² suggested that "flapping" of the shear layer due to the pairing between coherent structures caused the fluctuation in the reattachment.

2) Only the spectra measured inside the separation bubble, i.e., at $r_0 < r_r$, exhibited a peak at 520 Hz. Based on these observations, the following feedback mechanism is proposed. The coherent structures of the jets interact with the plates in the reattachment region. Pressure waves, generated by the interaction, propagate upstream and force the shear layer near the jet exit. Under forcing, the shear layer rolls up into coherent structures that are phase locked with the pressure

waves. This is the same model adopted to explain self-induced oscillations in flows interacting with solid boundaries.^{13,14} The resonant frequencies predicted by the model satisfy the following feedback equation⁵:

$$N = \frac{(r_r - r_j)}{(U_c/f)} + \frac{(r_r - r_j)}{(a_0/f)} \quad (5)$$

where U_c is the convection speed of the downstream-traveling coherent structures, which was measured by many researchers^{5,6} and is equal to approximately $0.65U$, $(r_r - r_j)$ is the characteristic length of the separation bubble, and $N=1,2,\dots$. According to Eq. (5), the conditions for resonance require that the summation of the downstream and upstream traveling waves along the feedback loop be equal to an integer N .

Equation (5) can be rewritten as

$$f = \frac{a_0}{(r_r - r_j)} \frac{N}{1 + (1/K_v M)} \quad (6)$$

where $K_v = U_c/U = 0.65$ and $M = 0.3$ is the jet Mach number.

Since the flow did not simultaneously reattach to both plates (see Fig. 4), the size of the separation bubble did not change significantly with H for $H > 10$ cm. The average reattachment radius was equal to 16 cm. Using this value for r_r , Eq. (6) predicts a value of $f = 518$ Hz, which is in excellent agreement with the measured frequency.

Conclusions

The impingement of two jets on each other was investigated experimentally. Each jet issued from a large flat plate. Flow visualization and surface pressure fluctuations indicated that strong jet oscillations occurred. However, the pressure fluctuations were axisymmetric when averaged over a time period larger than the characteristic time of jet oscillations. Pressure disturbances were generated due to the impingement of the jets and were amplified by feedback mechanisms. The high-frequency oscillation was amplified by acoustic reflection off the plates. The low-frequency oscillation, at approximately 220 Hz, was associated with a feedback of pressure waves between the impinging region and the open end of the flat plates. This oscillation lies in the frequency range of combustion instabilities measured in two-inlet, side-dump combustors,² which supports the hypothesis

that flow-induced oscillation may play a role in combustion instability.

Acknowledgment

The support of the U.S. Office of Naval Research (ONR) under Contract N0014-84-K-0373 is gratefully acknowledged.

References

- ¹Powell, A., "Aerodynamic Noise and the Plane Boundary," *Journal of the Acoustical Society of America*, Vol. 32, 1960, pp. 982-990.
- ²Waugh, R. C. et al., "A Literature Survey of Ramjet Combustor Instability," *Proceedings of ONR/AFOSR Workshop*, CPIA Pub. 375, 1983, pp. 1-13.
- ³Clark, W. H., "Experimental Investigation of Pressure Oscillations in a Side-Dump Ramjet Combustor," *Journal of Spacecraft and Rockets*, Vol. 19, Jan.-Feb. 1982, pp. 47-53.
- ⁴Clark, W. H., "Geometric Scale Effects on Combustion Instabilities in a Side Dump Liquid Fuel Ramjet," *19th JANNAF Combustion Meeting*, Vol. 1, CPIA Pub. 366, 1982, pp. 595-604.
- ⁵Ho, C. M. and Nossier, N. S., "Dynamics of an Impinging Jet. Part 1. The Feedback Phenomenon," *Journal of Fluid Mechanics*, Vol. 105, 1981, pp. 119-142.
- ⁶Neuwerth, G., "Acoustic Feedback Phenomena in Subsonic and Supersonic Free Jets that Strike a Perturbing Body," Dr. Ing. Thesis, Technische Hochschule Aschen, Aschen, FRG, 1973.
- ⁷Nossier, N. S. and Behar, S., "The Flowfield of a Side-Dump Combustor," *AIAA Journal*, Vol. 24, Nov. 1986, pp. 1752-1757.
- ⁸Kline, S. J., "On the Nature of Stall," *Transactions of ASME, Journal of Basic Engineering*, Vol. 81, 1959, pp. 305-320.
- ⁹Nossier, N. S., "Impinging Jets," *Encyclopedia of Fluid Mechanics*, Vol. 2, edited by N. P. Chermisinoff, Gulf Publishing Co., New York, 1986, Chap. 13.
- ¹⁰Wylie, C. R., *Advanced Engineering Mathematics*, 5th ed., McGraw-Hill, New York, 1982.
- ¹¹Troutt, T. R., Bhattacharjee, S., and Scheelke, B., "Modification of Vortex Interactions in a Reattaching Separated Flow," *Bulletin of the American Physical Society*, Vol. 29, No. 9, 1984, p. 1541.
- ¹²Eaton, J. K. and Johnston, J. P., "Turbulent Flow Reattachment: An Experimental Study of the Flow and Structure Behind a Backward Facing Step," Thermosciences Div., Stanford University, Stanford, CA, Rept. MD-39, 1980.
- ¹³Rockwell, D. and Naudascher, E., "Self-Sustained Oscillations of Impinging Free Shear Layer," *Annual Review of Fluid Mechanics*, Vol. 11, 1979, pp. 67-94.
- ¹⁴Jou, W. H. and Menon, S., "A Mechanism for the Acoustic-Vortex Interaction in a Ramjet Dump Combustor," *AIAA Paper* 86-1884, 1986.